Springer

KSME

Journal of Mechanical Science and Technology 32 (10) (2018) 4925~4931
www.springerlink.com/content/1738-494x(Print)/1976-3824(Online)
DOI 10.1007/s12206-018-0940-z

Unified model for the output accuracy of open-chain manipulators that considers joint clearance and structural parameters †

Shuwei Qu[1,2], Ruiqin Li[1,2,*], Shaoping Bai[3] and Shijie Liang[1]

[1]*School of Mechanical Engineering, North University of China, Taiyuan 030051, Shanxi, China*
[2]*Advanced Manufacturing Technology Key Laboratory of Shanxi Province, Shanxi, China*
[3]*Department of Mechanical and Manufacturing Engineering, Aalborg University, Aalborg, Denmark*

(Manuscript Received September 26, 2017; Revised May 26, 2018; Accepted July 3, 2018)

Abstract

A unified model is proposed for the output accuracy of open-chain manipulators in consideration of joint clearance and structural parameters. First, the operator of the finite-displacement screw matrix and the combination operation are presented. Second, the joint clearance and structural parameters are described and analyzed with screw theory. A virtual screw is established for the joint clearance and structural parameter errors. Third, a unified model is built through the adjoint transformation of Lie groups in consideration of the two effectors of the virtual screw. The error pose is decomposed into orientation and position errors, which are obtained through the virtual screw. Finally, an open-chain manipulator with six degrees of freedom is analyzed based on the proposed model. The position and orientation errors are obtained with the trajectory that provided an intuitive geometric insight into the accuracy and exact maximal position and orientation errors.

Keywords: Unified model; Output accuracy; Open-chain mechanism; Joint clearance; Structure parameters

1. Introduction

Output accuracy is a key issue in mechanism applications that is influenced various system elements, such as manufacturing tolerances, backlash, compliance, and active joint errors [1]. These elements can be classified as structural parameters and joint clearance.

Structural parameters are affected by deflection and manufacturing tolerance and cause a mechanism system to have a varying position and orientation. Elongated links are deformations that occur easily and seriously affect the output accuracy of manipulators [2, 3]. Output accuracy is considerably influenced by structural parameters and has been studied using statistical approaches [4-6]. The analytical method provides an accurate description of output accuracy given a change in structural parameters. However, recent studies have seldom examined this subject.

Joint clearance has an unpredictable, unrepeatable nature that leads to indeterminate effects on the manipulator's accuracy performance, and it cannot be compensated for by any type of calibration. Therefore, the effect of joint clearance on output accuracy has attracted the interest of many scholars. Joint accuracy analysis has been utilized by different researchers [7-12]. Chen et al. [13, 14] employed the geometric method to predict the accuracy performance effect of joint clearance and other factors. Intelligent algorithms have also been proposed for the inefficiency of joint clearance's influence on the output performance of manipulators due to the stochastic nature of joint clearance [15-17].

Generally, joint clearance and structural parameters that are assumed to be stochastic in nature are the primary sources that influence output performance. An effective and accurate approach must be developed to predict the effects of these error sources on the position and orientation deviation of manipulators. Kumaraswamy et al. [18] investigated a model for tolerance analysis that considers the invariance of links and joint clearance by referring to screw theory.

This work investigated these error sources in a unified manner with screw theory. The Denavit–Hartenberg (D–H) parameters were transformed into screw parameters. Joint clearance and structural parameter errors were presented through virtual screws. A unified model was built based on the adjoint transformation of Lie groups. The model was decomposed into orientation and position errors, which were obtained with a virtual screw. The output error was determined based on the trajectory that provided an intuitive geometric insight into accuracy performance and exact maximal position and orien-

*Corresponding author. Tel.: +86 3513921300, Fax.: +86 3513921300
E-mail address: liruiqin@nuc.edu.cn
† Recommended by Associate Editor Hugo Rodrigue

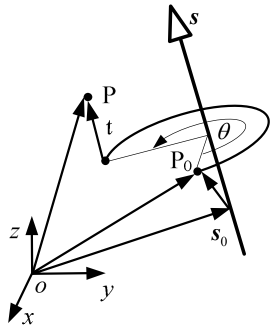

Fig. 1. Screw displacement of a rigid body.

tation errors. The model demonstrated high flexibility when used in kinematic analyses.

The remainder of this paper is organized as follows. The operator of the finite-displacement screw matrix and the combination operation are briefly introduced in Sec. 2. The error source and virtual screw are analyzed in Sec. 3. A unified model is built through the adjoint transformation of Lie groups in Sec. 4, and the pose error is decomposed with the virtual screw. The model is used to study the case of an open-chain manipulator with six degrees of freedom (DOF). The conclusions are presented in the last section.

2. Operator of the finite-displacement screw matrix and combination operation

2.1 Operator of the finite-displacement screw matrix

According to Chasles' theorem, the displacement of a rigid body can be regarded as a rotation about and a translation along an axis, as shown in Fig. 1. The direction of the screw axis is denoted by $\boldsymbol{s}=(s_x,s_y,s_z)$, and the position vector of a point lying on the screw axis is represented by $\boldsymbol{s}_o=(s_{ox},s_{oy},s_{oz})$ with respect to the global Cartesian coordinate system *o-xyz*. When point P on the rigid body rotates at angle θ about the axis and at translation distance *t* along the axis, parameters $\boldsymbol{s}$ and $\boldsymbol{s}_o$ and the screw parameters (θ,t) are referred to as Rodrigues parameters, which completely define the general displacement of the rigid body.

These parameters lead to the transformation matrix [19]. That is,

$$\mathbf{R}(\theta)+\varepsilon\mathbf{AR}(\theta)\,, \tag{1}$$

where

$$\mathbf{R}(\theta)=\begin{bmatrix} \mathrm{c}\theta+s_x^2(1-\mathrm{c}\theta) & s_y s_x(1-\mathrm{c}\theta)-s_z\mathrm{s}\theta & s_z s_x(1-\mathrm{c}\theta)+s_y\mathrm{s}\theta \\ s_y s_x(1-\mathrm{c}\theta)+s_z\mathrm{s}\theta & \mathrm{c}\theta+s_y^2(1-\mathrm{c}\theta) & s_y s_z(1-\mathrm{c}\theta)-s_x\mathrm{s}\theta \\ s_z s_x(1-\mathrm{c}\theta)-s_y\mathrm{s}\theta & s_y s_z(1-\mathrm{c}\theta)+s_x\mathrm{s}\theta & \mathrm{c}\theta+s_y^2(1-\mathrm{c}\theta) \end{bmatrix},$$

where c represents cos and s represents sin.

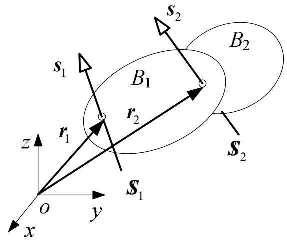

Fig. 2. Motion of the serial rigid body.

$$\mathbf{A}=[t\times]=\begin{bmatrix} 0 & -t_z & t_y \\ t_z & 0 & -t_x \\ -t_y & t_x & 0 \end{bmatrix},$$

where $\mathbf{R}$ is the primary part and $\mathbf{R}\in SO(3)$ represents the rotation about the axis. $\varepsilon\mathbf{AR}$ is the secondary part, and $\mathbf{A}$ is the skew–symmetry matrix representing the translation along the axis. The operator of the finite-displacement screw matrix can be arranged in form of a 6×6 screw matrix, that is,

$$\mathbf{N}=\begin{bmatrix} \mathbf{R} & \mathbf{0} \\ \mathbf{AR} & \mathbf{R} \end{bmatrix}. \tag{2}$$

The finite-displacement screw matrix is subject to the action of any identity screw, that is,

$$\boldsymbol{S}'=\mathbf{N}\boldsymbol{S}=\begin{bmatrix} \mathbf{R} & \mathbf{0} \\ \mathbf{AR} & \mathbf{R} \end{bmatrix}\begin{pmatrix} \boldsymbol{s} \\ \boldsymbol{s}_0 \end{pmatrix}=\begin{pmatrix} \mathbf{R}\boldsymbol{s} \\ \mathbf{AR}\boldsymbol{s}+\mathbf{R}\boldsymbol{s}_0 \end{pmatrix}=\begin{pmatrix} \mathbf{R}\boldsymbol{s} \\ [t\times]\mathbf{R}\boldsymbol{s}+\mathbf{R}\boldsymbol{s}_0 \end{pmatrix}, \tag{3}$$

where $\boldsymbol{S}=(\boldsymbol{s},\boldsymbol{s}_0)$ is an identity screw.

2.2 Combination operation of the finite-displacement matrix

In a serial manipulator, the motion imparted by the joints to the end-effector link can be represented by an ordered set of finite screw transformations. The first issue to consider is the distal joint in the serial chain, followed by the others toward the proximal joint. This ordered combination provides a resultant finite screw of the end effector relative to a datum location. In Fig. 2, two rigid bodies are connected by a revolute joint. The joint screws are $\boldsymbol{S}_1$ and $\boldsymbol{S}_2$, which can be represented by finite-displacement screw matrixes $\mathbf{N}_1$ and $\mathbf{N}_2$, respectively, as determined in Eq. (1) from the Rodrigues parameters. The motion of the end effector is the combination operation of the finite-displacement screw matrix. That is,

$$\mathbf{N}_1^2=\mathbf{N}_1\mathbf{N}_2\,. \tag{4}$$

3. Accuracy source analysis

3.1 Joint clearance error

The output performance of the mechanism is affected by joint clearance, as shown in Fig. 3. In the present work, the pin (shaft) and hole of the revolute pair were in accordance with

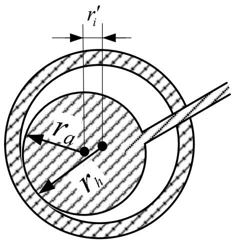

Fig. 3. Clearance error of the hole and pin.

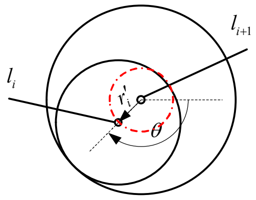

Fig. 4. Virtual screw of joint clearance.

the condition that contact was maintained all the time. That is, continuous contact of the revolute pair did not appear when the pin (shaft) was suspended in the hole. The size error of the hole and pin had a normal distribution, as shown in Fig. 3. Eccentricity can be regarded as infinitely small and has no weight virtual link r_i'; its angular position was 0° to 360° in this work because the contact between the pin and hole could occur anywhere along the circumference, as shown in Fig. 4. The eccentric distance is

$$r_i' = r_h - r_a \,, \tag{5}$$

where r_h is the dimension of the connecting accessory hole and r_a is the dimension of the connecting pin (shaft) caused by manufacturing tolerances, wear and tear from use, and other factors. According to the tolerances of the pin (shaft) and hole, the range is

$$\max r_i' = D^{ES} - d_{ei} \,, \tag{6}$$

$$\min r_i' = D_{EI} - d^{es} \,. \tag{7}$$

The virtual screw axis is along the joint axis direction, that is,

$$\boldsymbol{S}_{iv} = (\boldsymbol{s}_i, \boldsymbol{r}_i' \times \boldsymbol{s}_i) \,, \tag{8}$$

where $\boldsymbol{S}_{iv}$ is represented by the finite-displacement screw matrix and $\mathbf{N}_{iv}$ is determined as Eq. (1).

3.2 Structural parameter error

3.2.1 D–H structural parameters

The Denavit–Hartenberg convention provides a consistent and concise description of the kinematic relations between the links of a kinematic chain connected by lower pair joints with

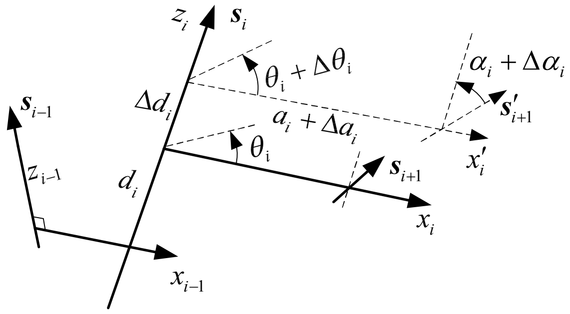

Fig. 5. Structural parameters.

one DOF. Four parameters are required to completely describe the relative pose of a link relative to its predecessor [20].

Links are numbered from 0 (base) to n (end effector). Joints are numbered from 1 to n. In this version of the procedure, joint i connects links i-1 and i. The local coordinate frame can be defined. z_i is the axis along joint i, origin o_i points along joint i and x_i is the common normal of z_i and z_{i+1}.

a_i is the distance between z_i and z_{i+1}, d_i is the distance between x_i and x_{i+1}, α_i is the angle between z_i and z_{i+1} measured along x_i and θ_i is the angle between x_i and x_{i+1} measured along z_i. The movement of link i+1 relative to its predecessor i connected by joint i is represented by screw $\boldsymbol{S}_i$, as shown in Fig. 5.

For each joint, the finite-displacement screw matrix parameters $\boldsymbol{s}$, $\boldsymbol{s}_o$, θ and t are identified together with the joint variable. The screw of the two ends for the ith link can then be obtained.

$$\boldsymbol{S}_i = [0,0,1;0,0,0]^T \,. \tag{9}$$

$$\boldsymbol{S}_{i+1} = \left[0, -s\alpha_i, c\alpha_i; 0, -a_i c\alpha_i, -a_i s\alpha_i\right]^T \,. \tag{10}$$

3.2.2 Expression of the structure parameter error by a virtual screw

The error of structural parameters a_i, α_i, θ_i and d_i are Δa_i, $\Delta\alpha_i$, $\Delta\theta_i$ and Δd_i, respectively, as shown in Fig. 5. The screws can be obtained from the change in the Plücker coordinate according to the relationship of the structural parameter error. The axis of Δa_i and $\Delta\alpha_i$ is coincident with the x_i axis. The screw pitch is $\Delta a_i / \Delta\alpha_i$. The kinematic screw is

$$\alpha_{xi}\boldsymbol{S}_{xi} = \Delta\alpha_i [1,0,0;\frac{\Delta\alpha_i}{\Delta a_i},0,0]^T \,. \tag{11}$$

The errors $\Delta\theta_i$ and Δd_i can be viewed as rotation angle $\Delta\theta_i$ and translation Δd_i along the z_i axis. The kinematic screw is

$$\theta_{zi}\boldsymbol{S}_{zi} = \Delta\theta_i [0,0,1;0,0,\frac{\Delta d_i}{\Delta\theta_i}] \,. \tag{12}$$

Therefore, the structural parameter can be represented by two virtual screws in the local coordinate parallel to x_i and z_i axes. The two virtual screws can also be represented by finite displacement screw matrix $\mathbf{N}_{ix}$ and $\mathbf{N}_{iz}$, respectively, as determined by Eq. (1).

4. Unified modeling of the output error

4.1 Adjoint transformation

Adg is an adjoint operator of Lie groups represented by **R** in *SO*(3) and a 4×4 matrix (**H**) or a 6×6 matrix (**N**) in *SE*(3).

We let the fixed coordinate system be **A**. Coordinate system B is obtained by applying pure rotation matrix **R** followed by translation matrix **A**. Therefore, the coordinate transformation from B to A is

$$\mathbf{N}=Adg(\mathbf{N})=\mathbf{N}_t\mathbf{N}_R=\begin{bmatrix}\mathbf{I} & \mathbf{0}\\ \mathbf{A} & \mathbf{I}\end{bmatrix}\begin{bmatrix}\mathbf{R} & \mathbf{0}\\ \mathbf{0} & \mathbf{R}\end{bmatrix}, \tag{13}$$

where $\mathbf{N}_t$ is the translation conversion matrix and $\mathbf{N}_R$ is the rotation conversion matrix.

4.2 Decomposition of the finite-displacement screw matrix

The finite-displacement screw matrix can be decomposed to a translation matrix form as $\mathbf{N}_t$ and to a rotation matrix form as $\mathbf{N}_r$. The motion of rotation about an arbitrary axis and translation along the axis can be interpreted in matrix forms as [21]

$$\mathbf{N}=\mathbf{N}_t\mathbf{N}_r=\begin{bmatrix}\mathbf{I} & \mathbf{0}\\ l\mathbf{A} & \mathbf{I}\end{bmatrix}\begin{bmatrix}\mathbf{R} & \mathbf{0}\\ [\boldsymbol{r}_e\times]\mathbf{R} & \mathbf{R}\end{bmatrix}. \tag{14}$$

4.3 Output performance of the open-chain manipulator

The reference coordinate frames for the extremity links are as follows: z_0 is located along the axis of joint 1, x_0 and y_0 are arbitrary, the x_n axis is normal to the joint n axis, and y_n and z_n are arbitrarily defined.

The output performance of the serial manipulator can be presented through successive adjoint transformation of Lie groups. That is,

$$^{n}\mathbf{P}_0(\theta)=\mathbf{N}_1\mathbf{N}_2\cdots\mathbf{N}_i\cdots\mathbf{N}_n\mathbf{P}(0). \tag{15}$$

The joint clearance and D–H parameter errors can be expressed through the virtual screw as Eqs. (8)-(10). According to the adjoint transformation of Eq. (2), each joint axis of the actual Plücker coordinates in the fixed coordinate system can be expressed as

$$\mathbf{N}_i'=\mathbf{N}_{ix}\mathbf{N}_{iz}\mathbf{N}_{iv}\mathbf{N}_i. \tag{16}$$

Therefore, the output performance of the open-chain manipulator can be presented as

$$^{n}\mathbf{P}_0'(\theta)=\mathbf{N}_1'\mathbf{N}_2'\cdots\mathbf{N}_i'\cdots\mathbf{N}_n'\mathbf{P}(0). \tag{17}$$

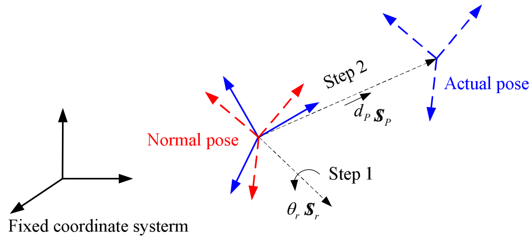

Fig. 6. Pose error of the end effector.

4.4 Analysis of the output accuracy of the end effector

The output performance of the manipulator was the pose of the end effector in this study.

Through coordinate system transformation, the error pose of the end effector was decomposed as the position and orientation, as shown in Fig. 6. The procedure involved three steps.

Step 1. The normal pose of the end effector in the global coordinate system was obtained through normal joint screw transformation, as shown in Eq. (15). The actual pose of the end effector in the global coordinate system was obtained as Eq. (17) by considering the joint clearance and structure parameter error.

Step 2. The actual orientation was obtained from the rotation of the normal coordinate system to the actual coordinate system of the end effector.

Step 3. The actual position was obtained through the translation of the normal coordinate system to the actual coordinate system of the end effector.

The pose error analysis procedure was equivalent to two virtual special screws. The first one was the orientation error, which was equivalent to an infinite-pitch screw. The second one was the position error, which was equivalent to a zero-pitch screw, as described in Fig. 6.

The orientation error and position screws are expressed as follows:

$$\theta_r\boldsymbol{S}_{vr}=\theta_r\begin{bmatrix}\boldsymbol{s}_r & \boldsymbol{s}_{rp}\end{bmatrix}^T, \tag{18}$$

$$d_p\boldsymbol{S}_{vP}=d_p\begin{bmatrix}0 & \boldsymbol{s}_{op}\end{bmatrix}^T, \tag{19}$$

where θ_r, $\boldsymbol{S}_{vr}$, $\boldsymbol{s}_r$ and $\boldsymbol{s}_{rp}$ are the orientation error, error screw axis, direction of the axes, and the moment for the original point, respectively.

d_p, $\boldsymbol{S}_{vP}$ and $\boldsymbol{s}_{op}$ are the position error, error screw axis, and position error, respectively.

Therefore, the relation of normal output performance to the actual output performance is

$$^{n}\mathbf{P}_0'(\theta)=d_p\boldsymbol{S}_{vp}\theta_r\boldsymbol{S}_{vr}\,{}^{n}\mathbf{P}_0(\theta). \tag{20}$$

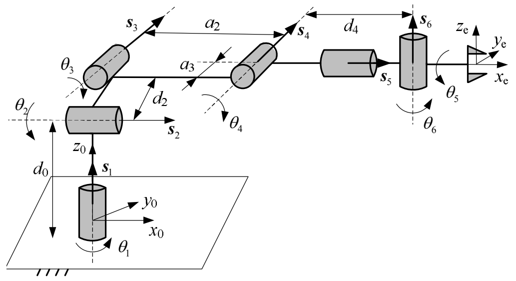

Fig. 7. Structure of the open-chain manipulator with 6 DOF.

The error is expressed as

$$\Delta\mathbf{P}(\theta) = d_p \boldsymbol{S}_{vp} \theta_r \boldsymbol{S}_{vr} \, {}^n\mathbf{P}_0(\theta) \, {}^n\mathbf{P}_0(\theta)^{-1} = {}^n\mathbf{P}_0'(\theta) \, {}^n\mathbf{P}_0(\theta) = \begin{bmatrix} \mathbf{R} & \mathbf{0} \\ \mathbf{AR} & \mathbf{R} \end{bmatrix} \tag{21}$$

$\mathbf{R} = \begin{bmatrix} r_{11} & r_{12} & r_{13} \\ r_{21} & r_{22} & r_{23} \\ r_{31} & r_{32} & r_{33} \end{bmatrix}$; therefore, $tr(\mathbf{R}) = r_{11} + r_{22} + r_{33}$.

The output orientation error is

$$\theta_r = \arccos\left(\frac{tr(\mathbf{R}) - 1}{2}\right). \tag{22}$$

If $\theta_r = 0$, no orientation error exists.
If $\theta_r \neq 0$, the orientation error in a different direction is

$$\boldsymbol{\omega}_r = \frac{1}{2\sin\theta_r} \begin{bmatrix} r_{32} - r_{23} \\ r_{13} - r_{31} \\ r_{21} - r_{12} \end{bmatrix}. \tag{23}$$

The position matrix is

$$\mathbf{A} = \mathbf{R}^{-1}\mathbf{AR}. \tag{24}$$

$\mathbf{A} = \begin{bmatrix} 0 & -t_z & t_y \\ t_z & 0 & -t_x \\ -t_y & t_x & 0 \end{bmatrix}$. Therefore, the position errors are

$$\begin{cases} p_x = t_x \\ p_y = t_y \\ p_z = t_z \end{cases}. \tag{25}$$

5. Simulation analysis

The 6-DOF open-chain manipulator consisted of a spherical arm and a spherical wrist. Its kinematic structure and screws are depicted in Fig. 7.

The joint screws were established according to Fig. 7, as shown Table 1. The structural parameters and structure parameter error are listed in Table 2.

Table 1. Joint screw of the open manipulator.

Screw	$\mathbf{s}_i$	$\mathbf{s}_{oi}$	θ_i	t_i
1	(0 0 1)	(0 0 0)	θ_1	0
2	(1 0 0)	$(0 - d_0\ 0)$	θ_2	0
3	(0 1 0)	$(d_0\ 0\ 0)$	θ_3	0
4	(0 1 0)	$(d_0\ 0 - a_2)$	θ_4	0
5	(1 0 0)	$(0 - d_0\ 0)$	θ_5	0
6	(0 1 0)	$(0\ a_2\ 0)$	θ_6	0

Table 2. Structural parameters of the 6-DOF open-chain manipulator.

Joint	θ /(°)	$\Delta\theta$ /(°)	d/mm	Δd /mm	a/mm	Δa /mm	α /(°)	$\Delta\alpha$ /(°)
1	0	0.1	0	0.02	0	0.02	0	0.1
2	90	−0.1	149	−0.02	431	−0.02	−90	−0.1
3	0	0.1	0	0.02	20	0.02	0	0.1
4	90	−0.1	433	−0.02	0	−0.02	90	−0.1
5	0	0.1	0	0.02	0	0.02	−90	0.1
6	0	−0.1	0	−0.02	0	−0.02	90	−0.1

Table 3. Tolerance of each joint.

Joint	1	2	3	4	5	6
Tolerance	[−0.035, 0.035]	[−0.027, 0.027]	[−0.132, 0.132]	0.02	0.02	0.02

The finite displacement matrix can be transformed according to the screw through Eq. (1). The error of the structural parameter can be replaced by the virtual screw through Eqs. (11) and (12).

Joint clearance can be obtained according to the tolerance of the structural parameters. The transition assembly was used in the manipulator system. The tolerance was obtained according to the structural parameters of the link. The tolerance level was 5. The tolerance of each joint is listed in Table 3.

In the original position, the coordinate frame of the end effector is parallel to the global coordinate frame. The distance in the three directions of x, y, z were 640, 149 and 920 mm, respectively. d_0 was 640 mm.

The position and the position error were obtained through Eqs. (15) and (25), respectively. The joint velocity was 10 mm/s, and the operation time was 60 s. The position error trajectory is shown in Fig. 8, and the position error is shown in Fig. 9.

Fig. 8 shows that the output position ranks in the three directions are [−500, 1500], [−1500, −500] and [−1100, 900]. Fig. 9 shows that the influence extent in the 3 directions is approximately [−9, 9], [9, 9] and [−17, 17], respectively. The relative output accuracies are 0.9 %, 1.8 % and 1.7 %. The output accuracies in the directions of y and z are higher than that in the x direction.

The output orientation trajectory and output orientation er-

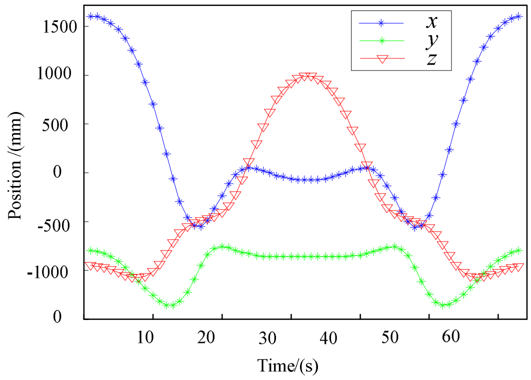

Fig. 8. Position trajectory of the mechanism.

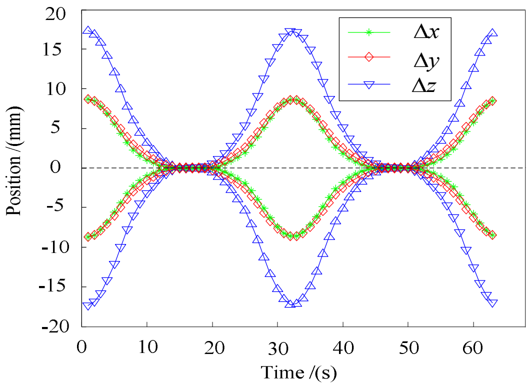

Fig. 9. Position output errors of the mechanism.

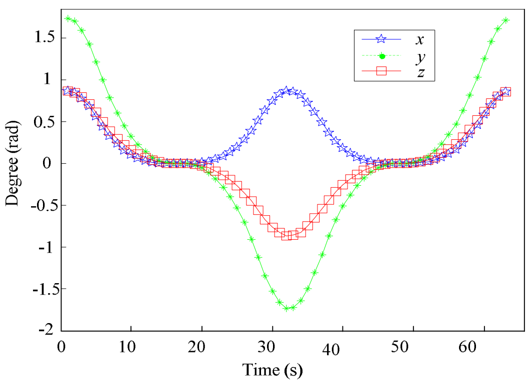

Fig. 10. Orientation trajectory of the mechanism.

rors can be obtained through Eqs. (15) and (23), respectively. The output orientation trajectories are shown in Fig. 10, and the output orientation errors are shown in Fig. 11.

Fig. 10 shows that the output orientations in the three directions are [0/rad, 1/rad], [−1.75/rad, 1.75/rad] and [−0.7/rad, 0.9/rad]. Fig. 11 shows that the influence extent in the three directions are approximately [−0.04/rad, 0.04/rad], [−0.06/rad, 0.06/rad] and [−0.06/rad, 0.06/rad], respectively. The relative output accuracies are 8 %, 3.4 % and 7.5 %. The output accuracy in the directions of x and z are higher than that in the y direction.

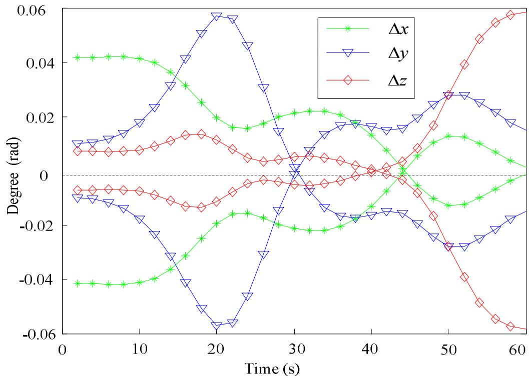

Fig. 11. Orientation output error of the mechanism.

6. Conclusions

A unified model for open-chain manipulators was proposed through an output accuracy analysis based on screw theory.

The operator of the finite-displacement screw matrix expressed any motion of the rigid body. All of the movements of the manipulator can be obtained based on the adjoint action.

Joint clearance can be assumed as a virtual screw. The D–H structural parameter error can be transformed into two virtual screws then combined with the adjoint action to build a unified model.

A 6-DOF open-chain manipulator was utilized for model implementation. The result verified the effectiveness of the model.

Acknowledgments

This work is supported by the National Natural Science Foundation of China (Grant No. 51275486) and Postgraduate Education Innovation Program of Shanxi Province (Grant No. 2016BY126).

Nomenclature

$\boldsymbol{s}$	: Direction of the screw axis
$\boldsymbol{s_0}$	: Position vector of the screw
$\mathbf{R}$	: Rotation matrix
$\mathbf{A}$	: Translation matrix
$\mathbf{N}$	: Finite displacement of the screw matrix
$\boldsymbol{\$}$	: Identity screw
r_i'	: Virtual link
r_h	: Dimension of the hole
r_a	: Dimension of the pin
D^{ES}	: Upper deviation of the hole
D_{EI}	: Lower deviation of the hole
d^{es}	: Upper deviation of the pin
d_{ei}	: Lower deviation of the pin
Adg	: Adjoint operator of the Lie group
$\mathbf{P}$	: Finial pose of the manipulator

References

[1] S. Briot and I. Bonex, Accuracy analysis of 3-DOF planar

parallel robots, *Mechanism and Machine Theory*, 43 (4) (2008) 445-458.
[2] L. Wang, Y. Jiang and T. Li, Running accuracy analysis of a 3-RRR parallel kinematic machine considering the deformations of the links, *Chinese Journal of Mechanical Engineering*, 27 (5) (2014) 890-899.
[3] Y. Yu, Z. Du, J. Yang and Y. Li, An experimental study on the dynamics of a 3-RRR flexible parallel robot, *IEEE Transactions on Robotics*, 27 (5) (2011) 992-997.
[4] J. Chakraborty, Synthesis of mechanical error in linkages, *Mechanism and Machine Theory*, 10 (2) (1975) 155-165.
[5] S. J. Lee, B. J. Gilmore and M. M. Ogot, Dimensional tolerance allocation of stochastic dynamic mechanical systems through performance and sensitivity analysis, *ASME Journal of Mechanical Design*, 115 (3) (1993) 392-402.
[6] L. Du, Y. Huang, C. Zou and M. Huang, Error modeling and simulation of open-chain linkage using virtual joint method, *Transaction of the Chinese Society Agricultural Machinery*, 26 (6) (2010) 157-162.
[7] A. Chaker, A. Mlika, M. A. Laribi, L. Romdhane and S. Zeghloul, Clearance and manufacturing errors effects on the accuracy of the 3-RCC spherical parallel manipulator, *European Journal of Mechanics A/Solids*, 37 (5) (2013) 86-95.
[8] J. Li, H. Huang, S. Yan and Y. Yang, Kinematic accuracy and dynamic performance of a simple planar space deployable mechanism with joint clearance considering parameter uncertainty, *Acta Astronautica,* 136 (2017) 34-45.
[9] K. Ting, J. Zhu and D. Watkins, The effects of joint clearance on position and orientation deviation of linkages and manipulators, *Mechanism and Machine Theory*, 35 (3) (2000) 391-401.
[10] Z. Zhao and J. Qiu, Motion and pointing error of AB axis for large radio telescope, *Mechanical Science and Technology for Aerospace Engineering*, 35 (4) (2016) 1-5.
[11] P. Xie, Y. Du and T. Xing, New error analysis method of mechanical system, *Computer Engineering and Applications*, 47 (1) (2011) 36-39.
[12] X. Wang, G. Liu and S. Ma, Dynamic analysis of planar mechanical systems with clearance joints using a new nonlinear contact force model, *Journal of Mechanical Science and Technology*, 30 (4) (2016) 1537-1545.
[13] G. Chen, H. Wang and Z. Lin, Generalized kinematic mapping of constrained plane motions and its application to the accuracy analysis of general planar parallel robots, *Mechanism and Machine Theory*, 50 (2) (2012) 29-47.
[14] G. Chen, H. Wang and Z. Lin, A unified approach to the accuracy analysis of planar parallel manipulators both with input uncertainties and joint clearance, *Mechanism and Machine Theory*, 64 (6) (2013) 1-17.
[15] D. Sun and G. Chen, Kinematic accuracy analysis of planar mechanisms with clearance involving random and epistemic uncertainty, *European Journal of Mechanics A/Solids*, 58 (2016) 256-261.
[16] H. Wang, G. Chen, Y. Zhao and Z. Lin, Output error bound prediction of parallel manipulators based on the level set method, *Mechanism and Machine Theory*, 45 (8) (2010) 1153-1170.
[17] L. Ramesh Kumar, K. P. Padmanaban, S. Ganesh Kumar and C. Balamurugan, Design and optimization of concurrent tolerance in mechanical assemblies using bat algorithm, *Journal of Mechanical Science and Technology*, 30 (6) (2016) 2601-2641.
[18] U. Kumaraswamy, M. Shunmugam and S. Ujatha, A unified framework for tolerance analysis of planar and spatial mechanisms using screw theory, *Mechanism and Machine Theory*, 69 (6) (2013) 168-184.
[19] J. Dai, *Geometrical foundations and screw algebra for mechanisms and robotics*, Higher Education Press, Beijing (2014).
[20] C. Rocha, C. Tonetto and A. Dias, A comparison between the Denavit-Hartenberg and the screw-based methods used in kinematic modeling of robot manipulators, *Robotics and Computer-Integrated Manufacturing*, 27 (4) (2011) 723-728.
[21] J. S. Dai, Finite displacement screw operators with embedded chasles' motion, *Joural of Mechanisms and Robotics*, 4 (4) (2012) 041002.

Shuwei Qu was born in 1978 and is currently a Ph.D. candidate at the School of Mechanical Engineering, North University of China. Her research interests include robotics and mechanism theory of parallel manipulators. E-mail: shuweiqu1222@nuc.edu.cn.

Ruiqin Li was born in 1964 and is currently a Professor and Ph.D. supervisor at the School of Mechanical and Power Engineering, North University of China. She received her Ph.D. degree from Shanghai Jiao Tong University in 2004. She was a senior visiting scholar at King's College in London, UK. Her research interests include mechanism and robot theory and complex mechanical system design. E-mail: liruiqin@nuc.edu.cn.